J. Sci. I. R. Iran

Vol.10 No.1
Winter 1999

STUDY OF NUCLEAR LEVEL DENSITY AND SPIN CUT-OFF FACTORS

A.N. Behkami and Z. Kargar

Department of Physics, Shiraz University, Shiraz, Islamic Republic of Iran

Abstract

Nuclear level densities and spin cut-off factors have been deduced for nuclei in the mass region $24<A<63$, from a microscopic theory, which includes nuclear pairing interaction. Single particle levels for both Seeger and Nilsson potentials were used in the calculations. Level densities extracted from the theory are compared with their corresponding experimental values. It is found that the overall agreement between experimental level densities and the microscopic theory with pairing is very good. The calculational procedure to account for an odd particle system blocking, as well as the effect of such blocking, is also discussed.

1. Introduction

In all statistical theories the nuclear level density is the most characteristic quantity and plays an essential role in the study of nuclear structure. The Fermi gas model [1] has often been used in the study of statistical treatment of nuclear properties.

However, computation of level density parameter 'a' from neutron resonance data using a noninteracting model shows marked shell effects [2]. The use of single particle levels obtained from the shell model calculation in the evaluations of nuclear state densities has been discussed by various authors [3,4].

Furthermore, the superconductivity theory [5] predicts the existence of the transition energy, below which the Fermi gas model is invalidated. In fact in this superconducting phase the energy temperature relation is much different from that expected from the later model and the level density is much smaller than is expected by the extrapolation from normal phase. In this way the prediction of the low energy behaviour of level densities has been much improved [6].

Since detailed and high resolution (n, γ) and transfer reaction data has become available, the authors have considered it worthwhile to apply the statistical approach to examine the effects of BCS pairing interaction in order to see to what extent the pairing interaction is needed to give agreement between measured and calculated level densities. In addition we would like to find out what influence the discrete structure of single particle spectra has on the behaviour of the nuclear and state densities, and whether one set of single particle energies is better than another for calculating level densities. In section 2 the general theory will be discussed, in section 3 the actual calculational procedure will be presented and in section 4 the results obtained will be compared with their corresponding experimental values and discussed.

Keywords: Nuclear level densities for light A nuclei

2. Level Density Formulas

Consider a system of nucleons interacting with the pairing force. For a spherically symmetric nuclei, in addition to being characterized by energy ε_k, the single fermion states are also characterized by the projection of the angular momentum on the z-axis, m_k. In the superconducting theory, the nucleons having angular momentum (m_k, - m_k) couple so as to form a quasi bound particle.

The state density of such an N nucleon system of

energy E is related to the logarithm of the grand partition function [7],

$$\Omega(\alpha, \beta) = -\beta\sum_k (\varepsilon_k-\lambda-E_k)+ 2\sum_k ln[1+exp(-\beta E_k)]-\beta\frac{\Delta^2}{G} \quad (1)$$

where α and β are two Lagrangian multipliers associated with the nucleon number and energy, $E_k=[(\varepsilon_k-\lambda)^2+\Delta^2]^{1/2}$ is the quasi particle energy, ε_k the single particle energy, Δ the gap parameter, $\lambda=\alpha/\beta$ is the chemical potential and G is the strength of pairing.

The quantities Δ, λ and $\beta(=1/T$, T is the nuclear temperature) are connected through the following gap equation:

$$\frac{2}{G}=\sum_k \frac{1}{E_k} tanh\frac{\beta E_k}{2} \quad (2)$$

The summation is over doubly degenerate orbitals designated by 'k'.

The state density is the inverse transform of the grand partition function,

$$\omega(N, E)=(\frac{1}{2\pi i})^2 \oint d\alpha \oint d\beta Z(\alpha, \beta)\, exp\,(-\alpha N+\beta E) \quad (3)$$

The above contour integrals can be evaluated by the method outlined previously [8-10], the result is:

$$\omega(N, E)=\frac{exp(S)}{2\pi D^{1/2}} \quad (4)$$

here the entropy S can be written as:

$$S=2\sum_k ln[1+exp(-\beta E_k)]+ 2\beta\sum_k \frac{E_k}{1+exp\,(\beta Ek)} \quad (5)$$

and 'D' is a 2×2 determinant with its elements given in terms of the second derivations of the grand partition function.

The statistical properties of a nucleus defined in terms of the nuclear number N and energy E are given by:

$$N=\frac{1}{\beta}\frac{\partial lnZ}{\partial\lambda}=\sum_k n_k \quad (6)$$

$$E=\frac{-\partial lnZ}{\partial\beta}=\sum_k \varepsilon_k n_k-\frac{\Delta^2}{G} \quad (7)$$

where the occupation probability n_k is given by

$$n_k = 1-\frac{\varepsilon_k-\lambda}{E_k} tanh\frac{\beta E_k}{2} \quad (8)$$

The statistical properties of a nucleus is defined in terms of its neutron and proton numbers N and Z and the total energy E. Because of the additive properties of energy and nucleon number, we can extend the above derivation to include a nuclear system. For a nucleus of N neutrons of energies ε_{nk} with magnetic quantum numbers m_{nk} and Z protons of energies ε_{pk} with magnetic quantum numbers m_{pk}, the constants of motion are then neutron and proton numbers given by (6) and the total energy $E=E_p+E_n$ given by (7).

The total state density for a system of N neutrons and Z protons at an excitation energy $U=U_p+U_n$ is

$$\omega(N, Z, U)=\frac{exp(S)}{(2\pi)^{3/2}D^{1/2}} \quad (9)$$

here $S=S_n+S_p$ is the total entropy and 'D' is now a 3×3 determinant.

Finally, the total level density for a nuclear system at an excitation energy $U=E-E_{ground}$ is given by

$$\rho(N, Z, U)=\omega(N, Z, U)/(2\pi\sigma^2)^{1/2} \quad (10)$$

where σ^2 is the total spin cut-off parameter defined as:

$$\sigma^2=\sigma_n^2+\sigma_p^2$$

with

$$\sigma_n^2=\frac{1}{2}\sum_k m_{nk}^2\, sinh^2\,(\frac{1}{2}\beta E_{nk}) \quad (11)$$

and a similar relation for σ_p^2, where ε_{nk} and m_{nk} are the single particle energies and magnetic quantum numbers respectively.

3-1. Energy Gap and Critical Temperature

In view of the importance of the pairing energy in nuclear level density, we have calculated its dependence on nuclear temperature. For a nuclear system characterized by its single particle energies ε_k and magnetic quantum numbers m_k, calculations are done in the following way. (i) At zero temperature, Equations 2 and 6 are solved for $\lambda(0)$ and the pairing strength G for known particle number N and gap parameter Δ. The initial values of gap parameters were obtained from the newest mass table of Audi *et al.* [11]. (ii) The critical temperature, T_c, and the corresponding chemical potential, λ_c, are evaluated by setting $\Delta=0$ and

solving the same equations for specified nucleon number N and pairing strength G. (iii) The quantities $\lambda(T)$ and $\Delta(T)$ are then evaluated for a given value of T by solving (2) and (6) with the values of N and G from (i). These values of $\lambda(T)$ and $\Delta(T)$ are used to compute other thermodynamic quantities which will be discussed in the following sections.

It is worth noting that the pairing strength G depends on the number of single particle levels which are included in the calculation. However, for a given value of Δ the final results are not sensitive to the number of single particle levels as long as sufficient levels are included so that the levels of largest 'k' have very small occupational probabilities. Temperature dependence of the energy gap parameters for both the neutron and proton systems for ^{56}Fe nucleus are shown in Figure 1. It is seen from this figure that the energy gap parameter decreases rapidly with increasing temperature and vanishes altogether at the critical temperature.

3-2. Excitation Energy and Entropy

The excitation energy of the nuclear system with temperature T can be evaluated as follows: (i) the intrinsic energy of the ground state, $E_n(0)$ is obtained from (7) for known values of $\lambda(0)$ and G obtained in section 3-1. In the same way, the intrinsic energy $E_n(T)$ is obtained from known values of $\lambda(T)$ and $\Delta(T)$ obtained again in section 3-1. Thus, the excitation energy of the neutron system at temperature T is given by $U_n = E_n(T) - E_n(0)$. The excitation energy of the proton system is obtained in the same way, $U_p = E_p(T) - E_p(0)$, thus the total excitation energy at temperature T is $U = U_n + U_p$.

The excitation energy for the neutron and proton systems for ^{56}Fe nucleus is plotted as a function of temperature in Figure 2. The arrows indicate the energies of the phase transition from the superconducting state to the normal state. By examining this figure we see that the functional relationship of the excitation energy and temperature is quite different above and below the critical temperature.

The entropy of the neutron and proton systems is evaluated from Equation 5 at temperature T from the values of $\lambda(T)$ and $\Delta(T)$ obtained in section 3-1. From the additivity property of entropy, the total entropy is obtained as $S = S_n + S_p$. The entropies are plotted as a function of temperature in Figure 3 for ^{56}Fe nucleus. Again the arrows indicate the phase transition from superconducting state to the normal state.

The calculational procedure just outlined is for even particle systems where the index 'k' sums over doubly degenerate levels.

3-3. Odd Particle Systems

For an odd particle system, blocking is important and must be included. When a level near the Fermi surface is occupied by an odd particle, the effect of the pairing

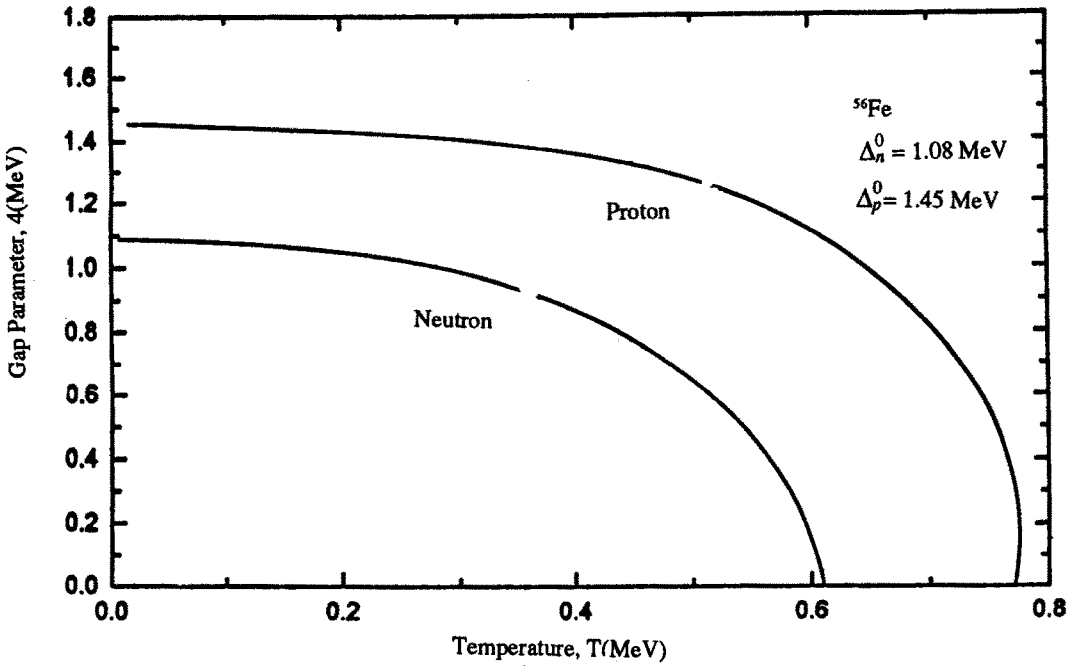

Figure 1. Temperature dependence of the neutrons and protons gap parameters for ^{56}Fe. $\Delta_n(T=0) = 1.08$ MeV and $\Delta_p(T=0) = 1.45$ MeV

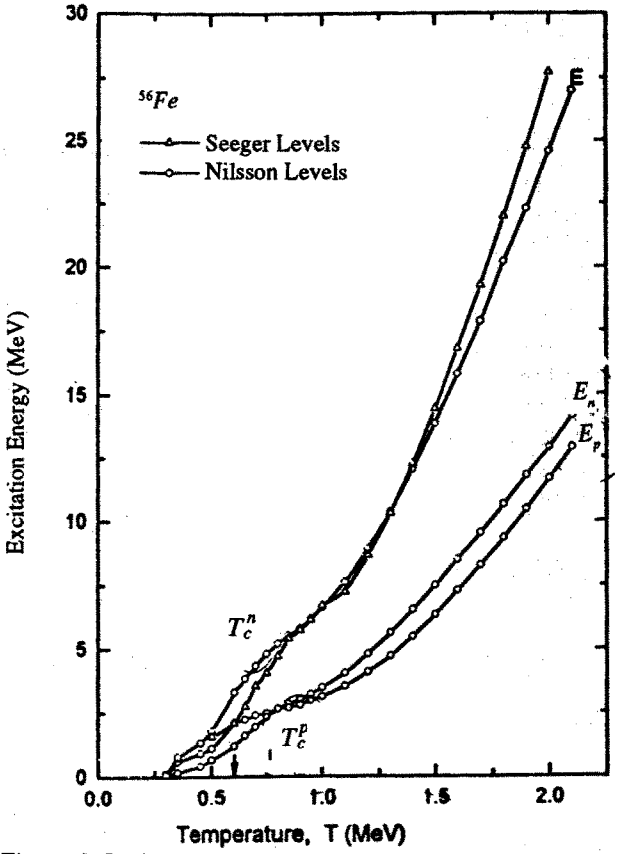

Figure 2. Intrinsic excitation energy for ^{56}Fe is plotted as a function of the temperature

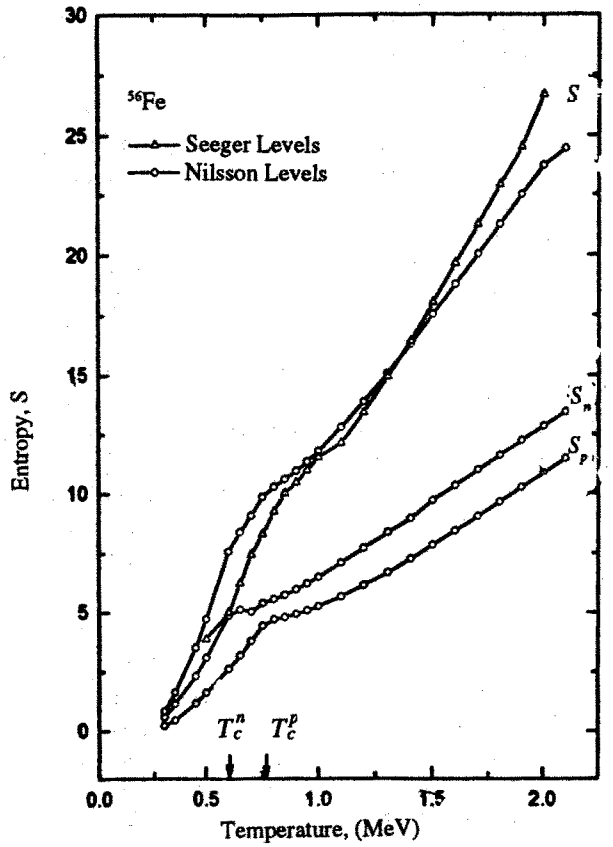

Figure 3. Relation between the entropy, S, and nuclear temperature, T(MeV), for ^{56}Fe. The arrows indicate the neutron and proton critical temperature.

correlation is reduced. The reduction necessary depends on which level is occupied. The change in Δ between the even and odd case due to the blocking of one level by the odd particle is estimated as [10],

$$\Delta^{odd}(0) \simeq \Delta^{even}(0) - \frac{1}{(\Delta^{even}(0))^2}\left(\sum_{k \neq k'} \frac{1}{E_k^3}\right)^{-1} \qquad (12)$$

where k′ indicates a state occupied by the odd particle. The actual calculation, in which the blocking effect has been included, indicates a difference in Δ between the even and odd system of the order of 20%. These results are roughly in agreement with Equation 12.

We have investigated the blocking effect by two different methods. (i) By reducing the strength of pairing parameter Δ. The change in Δ leads to a change in the in Δ, the odd particle system is treated in a way analogous to the even particle system. (ii) By adjusting the ground state for nuclear pairing. The statistical functions here were calculated from the adjacent doubly even nucleus and then the energy scale was shifted by an energy equivalent to that required to produce one quasi-particle. It turns out that the results of both procedures give generally identical level densities especially at higher excitation energies. This will be shown in the next section.

3-4. Nuclear State and Level Density

In performing calculations of state and level density, the energies and spins of the single particle levels were first calculated with a program and parameters of Nilsson *et al.* [12]. The quantities χ and μ which enter the Nilsson potential were taken from reference [12]. The relative energies and spins obtained from a Seeger program for two of the nuclei ^{56}Fe and ^{60}Ni for twenty-eight doubly degenerate levels are given in Table 1 and for ^{56}Fe they are displayed in Figure 4. Note that the Fermi energies are indicated for neutron and proton components. In actual calculation however, many more single particle levels were introduced.

Next the values of E_n, S_n and $\omega(N, U_n)$ were calculated from (7), (5) and (4) using the values of $\lambda(T)$ and $\Delta(T)$ obtained in section 3-1. The spin cut-off factor σ_n^2 is calculated using (11) from the known values of eigenvalues ε_{nk} and their corresponding magnetic quantum numbers

Table 1. Relative energies of single particle level of Seeger for ^{56}Fe and ^{60}Ni

	^{56}Fe				^{60}Ni			
K	State	Neutron Energy	State	Proton Energy	State	Neutron Energy	State	Proton Energy
1	$1s_{1/2}$	0.00	$1s_{1/2}$	0.00	$1s_{1/2}$	0.00	$1s_{1/2}$	0.00
2	$1p_{3/2}$	8.07	$1p_{3/2}$	7.52	$1p_{3/2}$	7.89	$1p_{3/2}$	7.27
3		8.07		7.53		7.89		7.27
4	$1p_{1/2}$	12.20	$1p_{1/2}$	10.74	$1p_{1/2}$	11.93	$1p_{1/2}$	10.38
5	$1d_{5/2}$	16.38	$1d_{5/2}$	14.97	$1d_{5/2}$	16.01	$1d_{5/2}$	14.47
6		16.38		14.97		16.01		14.47
7		16.38		14.97		16.01		14.47
8	$2s_{1/2}$	20.59	$1d_{3/2}$	19.23	$2s_{1/2}$	20.13	$1d_{3/2}$	18.59
9	$1d_{3/2}$	21.85		19.23	$1d_{3/2}$	21.35		18.59
10		21.85	$2s_{1/2}$	19.83		21.35	$2s_{1/2}$	19.17
11	$1f_{7/2}$	24.75	$1f_{7/2}$	22.32	$1f_{7/2}$	24.19	$1f_{7/2}$	21.57
12		24.75		22.32		24.19		21.57
13		24.75		22.32		24.19		21.57
14		24.75		22.32		24.19		21.57
15	$2p_{3/2}$	29.43	$1f_{5/2}$	27.34	$2p_{3/2}$	28.76	$1f_{5/2}$	26.42
16		29.43		27.34		28.76		26.42
17	$1f_{5/2}$	31.20		27.34	$2f_{5/2}$	30.50		26.42
18		31.20	$2p_{3/2}$	28.20		30.50	$2p_{3/2}$	27.26
19		31.20		28.20		28.29		27.26
20	$2p_{1/2}$	32.20	$1g_{9/2}$	29.56	$2p_{1/2}$	31.47	$1g_{9/2}$	28.57
21	$1g_{9/2}$	33.11		29.56	$1g_{9/2}$	32.36		28.57
22		33.11		29.56		32.36		28.57
23		33.11		29.56		32.36		28.57
24		33.11		29.56		32.36		28.57
25		33.11	$2p_{1/2}$	30.37		32.36	$2p_{1/2}$	29.35
26	$2d_{5/2}$	38.20	$1g_{7/2}$	35.20	$2d_{5/2}$	37.34	$1g_{7/2}$	34.03
27		38.20		35.20		37.34		34.03
28		38.20		35.20		37.34		34.03

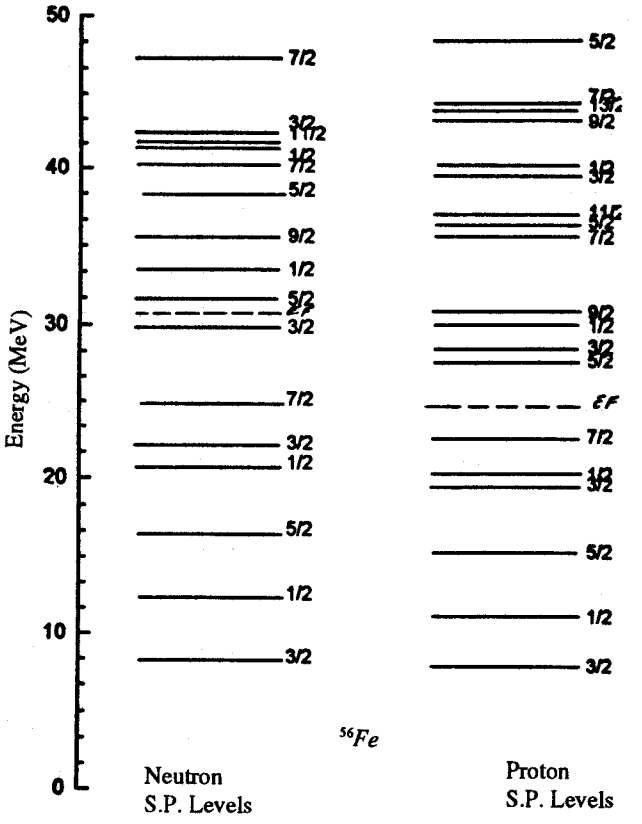

Figure 4. Energies of Nilsson single particle levels for 20 doubly degenerate levels with their spins

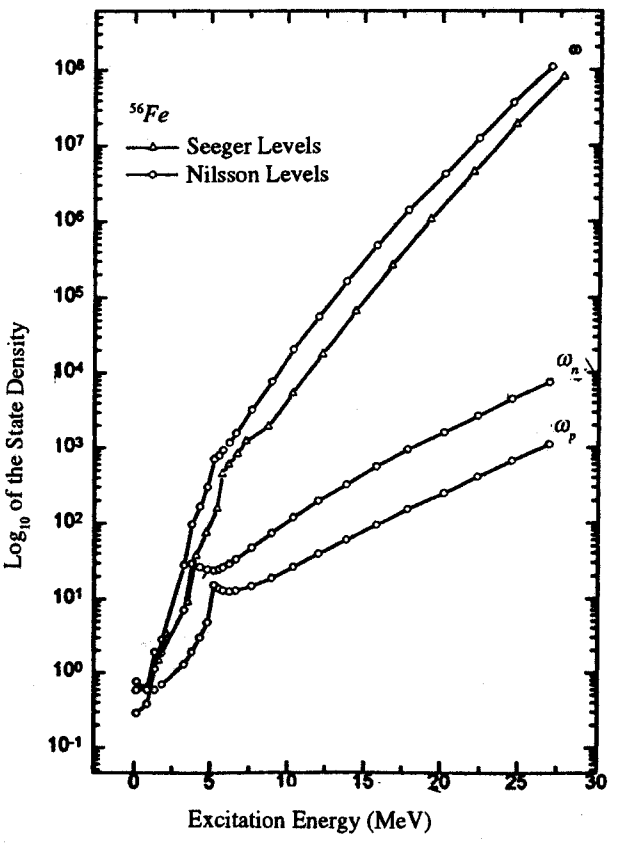

Figure 5. The logarithm of the state density as a function of excitation energy for ^{56}Fe, with the levels of Seeger *et al.* [16] and Nilsson *et al.* [12]

m_{nk}. Then the calculations are repeated for proton component. Finally, the quantities σ^2, $\omega(N, Z, U)$ and $\rho(N, Z, U)$ are calculated with (11), (9) and (10), the total excitation energy $U = U_n + U_p$. In Figure 5 the logarithm of the state density is plotted as a function of excitation energy for ^{56}Fe nucleus. Again the effect of pairing energy and shell effect is quite apparent at lower energies.

3-5. Spin Cut-off Factor

Spin cut-off factor σ^2 is usually determined by counting the levels with given spins and by fitting the spin distribution with

$$F(J) = exp\left(\frac{-J^2}{2\sigma^2}\right) - exp\left(\frac{-(J+1))^2}{2\sigma^2}\right) \qquad (13)$$

Some preliminary results have been presented in our previous paper [13]. In the present calculation, the spin cut-off factor is calculated with the microscopic theory from the known values of the single fermion energies ε_k and their corresponding magnetic quantum number m_k. This is done using [14]

$$\sigma^2 = \frac{1}{2}\{\sum_k m_{nk}^2 sinh^2(\frac{1}{2}\beta E_{nk}) + \sum_k m_{pk}^2 sinh^2(\frac{1}{2}\beta E_{pk})\} \qquad (14)$$

which is made up of the sum of the neutron and proton components.

We have compared the results with those obtained on the basis of the macroscopic theory given by [15]

$$\sigma^2 = 0.0888atA^{2/3} \qquad (15)$$

where the nuclear temperature, t, is related to excitation energy through (16),

$$U = at^2 - t \qquad (16)$$

here 'a' is the level density parameter. The value of $a = \frac{A}{8}$ is used in the present calculation.

In Figure 6 we show the variation of σ_n^2, σ_p^2 and σ^2 with excitation energy determined from the microscopic theory for the case of ^{60}Ni nucleus. The results from the macroscopic theory are also shown for comparison. We

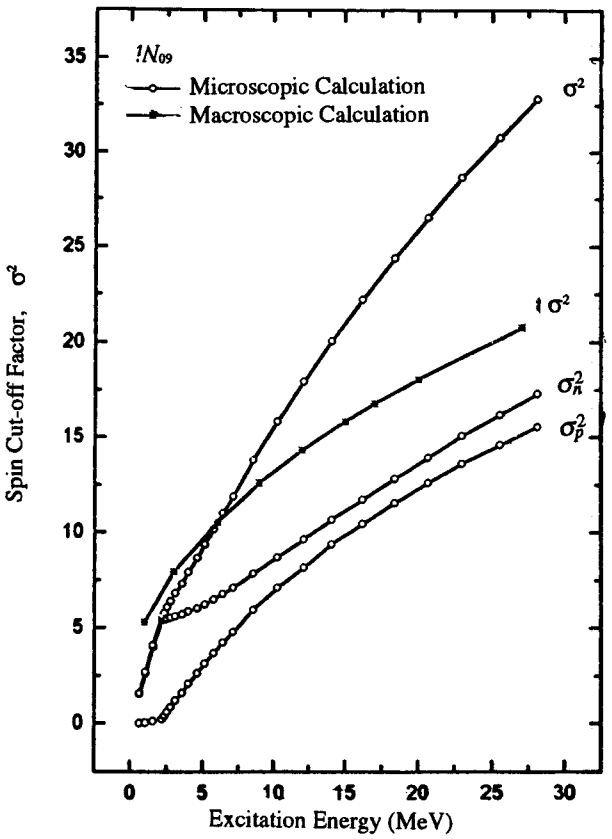

Figure 6. The spin cut-off factor for ^{60}Ni with a microscopic theory including the nuclear pairing interaction. The macroscopic calculations are also shown for comparison.

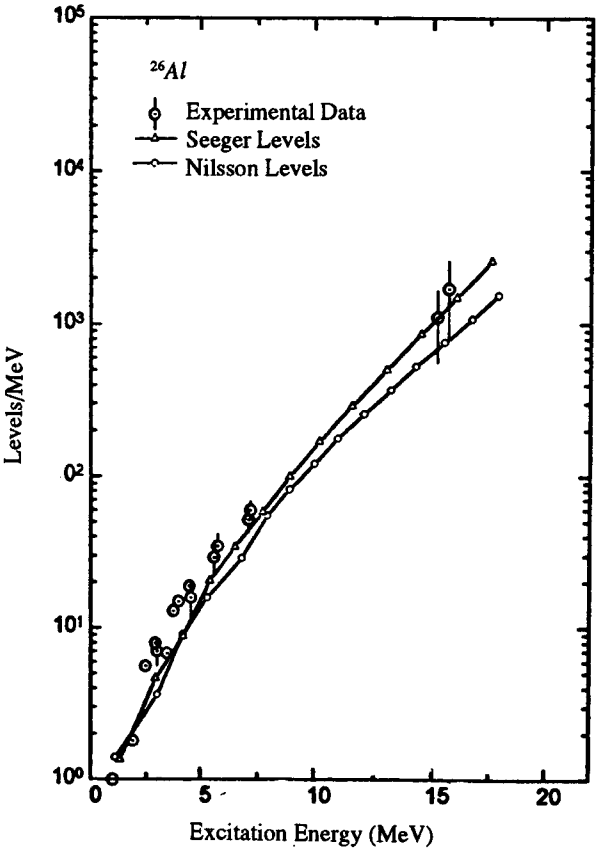

Figure 7. Comparison of the experimental level density of ^{26}Al with a microscopic theory including the nuclear pairing interaction, the theoretical calculations were performed with the single particle levels of Seeger *et al.* [16] and Nilsson *et al.* [12]. The experimental data was taken from M. Beckerman [18] and A.S. Ilijnov *et al.* [17].

see the role of the nuclear structure effect is quite apparent; this will be discussed in the following section.

4. Results and Discussion

We have computed the nuclear level densities in levels per MeV and spin cut-off factors for all nuclei with $24<A<63$. Here we present comparisons of level densities from microscopic theory and experiment for $^{26}_{13}Al$, $^{28}_{14}Si$, $^{33}_{16}S$, $^{38}_{18}Ar$, $^{41}_{20}Ca$, $^{56}_{26}Fe$ and $^{60}_{28}Ni$. The results of these comparisons are shown in Figures 7-13. Two different sets of single particle levels are used in the theoretical calculations, one set is due to Seeger and Parisho [16] and the other to Nilsson and coworkers [12].

The initial values of Δ_n and Δ_p for the even-even nuclei were taken from the literature [11] and then adjusted to improve the fit to the data. The final values of the pairing parameters for doubly even nuclei given in Table 2 were used for both the Seeger and Nilsson single particle levels.

The level density of the odd A nuclei was obtained using the procedure outlined in section 3-3. For example the level density of ^{33}S is obtained from the level density of ^{32}S by shifting the energy scale by Δ_n= 2.39 MeV. A similar level density is obtained by calculating Δ_n^{odd} (0) from Equation II and doing the calculation for ^{33}S.

Table 2. Proton and neutron pairing parameters used in the level density calculation

Nucleus	Δ_p(MeV)	Δ_n(MeV)
$^{28}_{14}Si$	2.28	2.18
$^{32}_{16}S$	2.50	2.39
$^{38}_{18}Ar$	2.06	2.20
$^{56}_{26}Fe$	1.45	1.08
$^{60}_{28}Ni$	0.91	0.86

As can be seen from Figures 7-13, the overall agreement between the experimental level densities and the microscopic theory with pairing is very good for both the

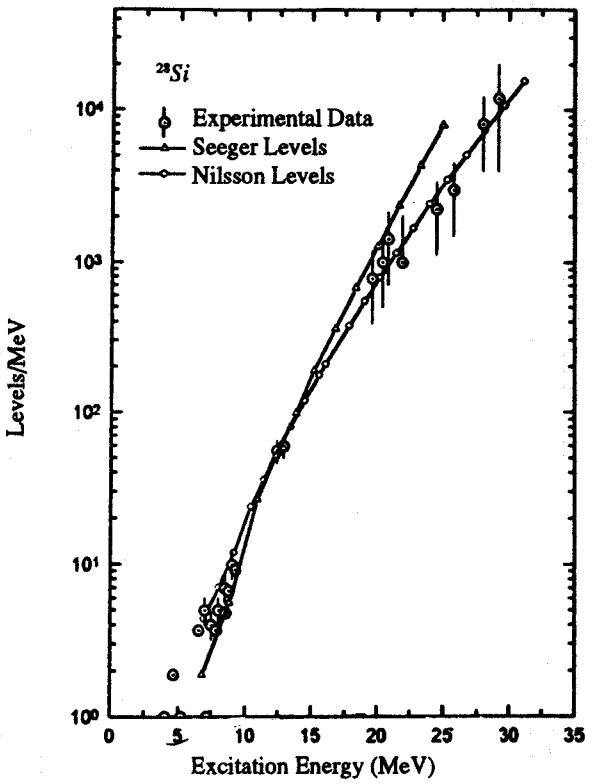

Figure 8. Same as Figure 7 for ^{28}Si

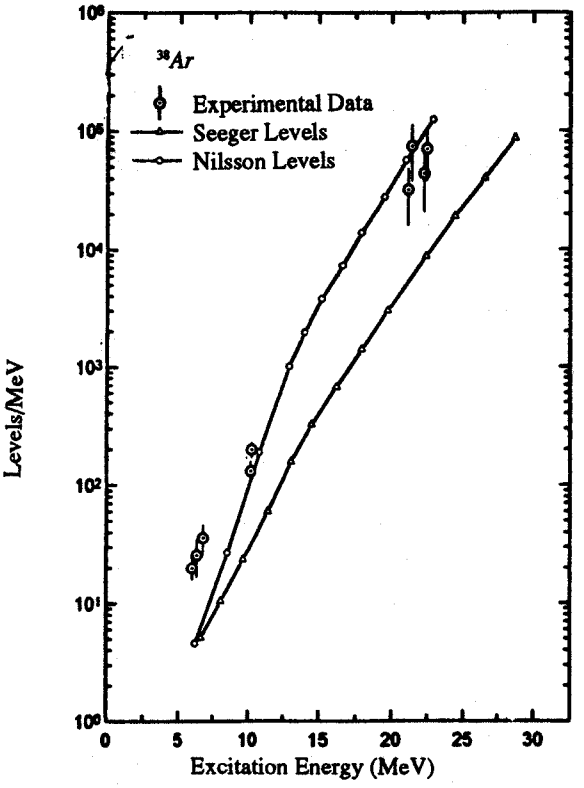

Figure 10. Same as Figure 7 for ^{38}Ar

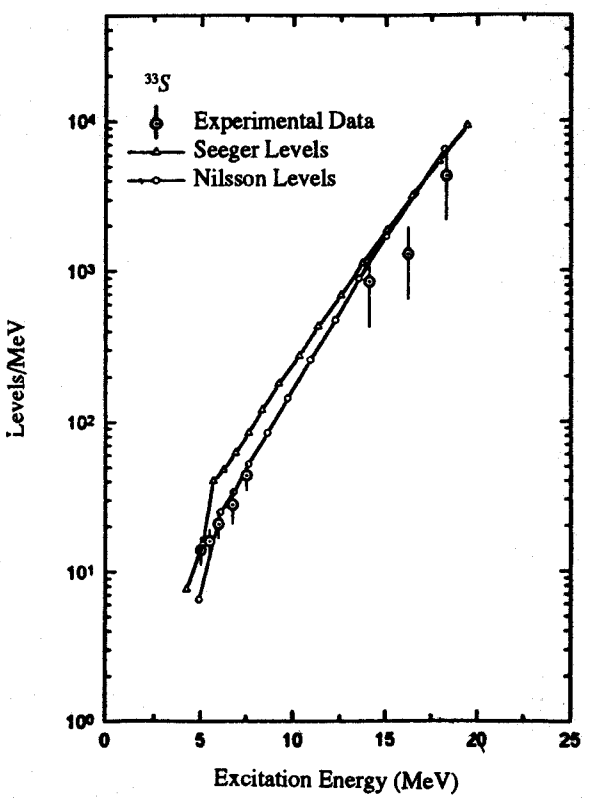

Figure 9. Same as Figure 7 for ^{33}S

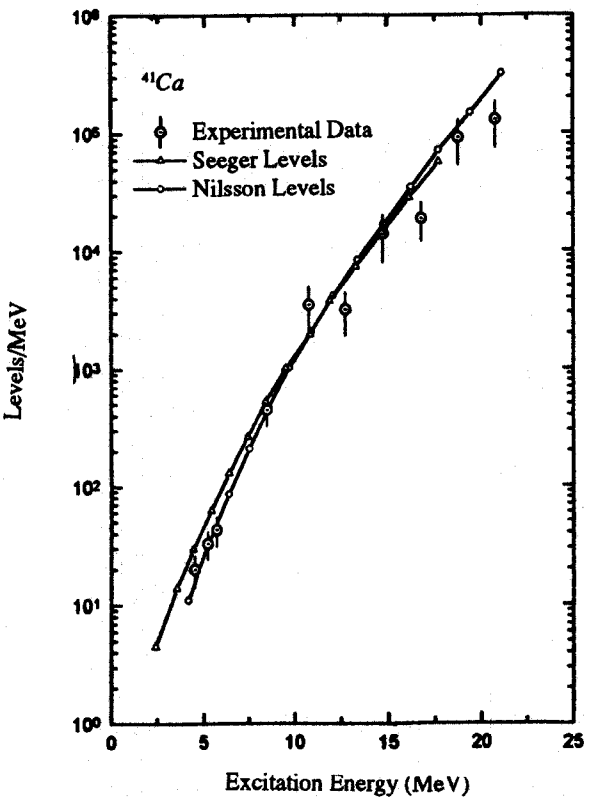

Figure 11. Same as Figure 7 for ^{41}Ca

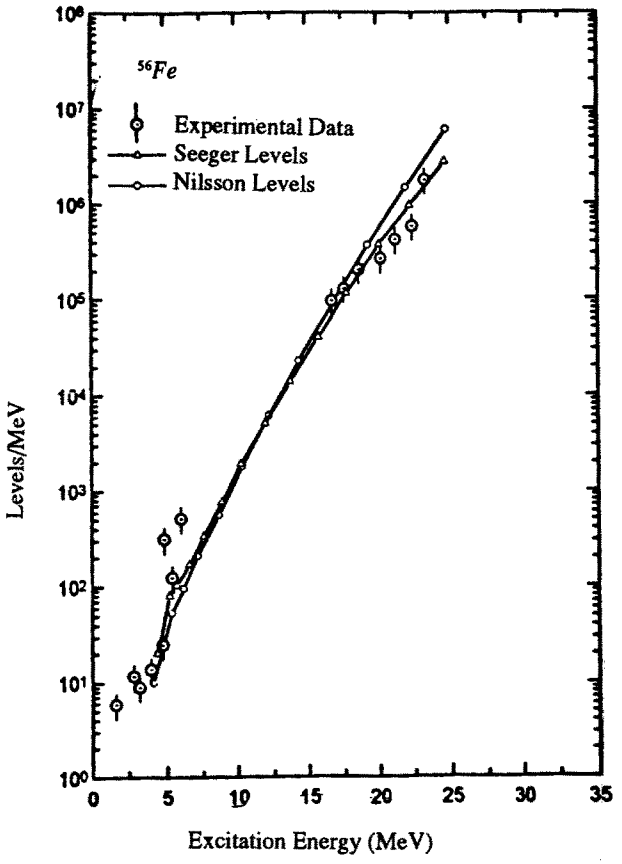

Figure 12. Same as Figure 7 for ^{56}Fe

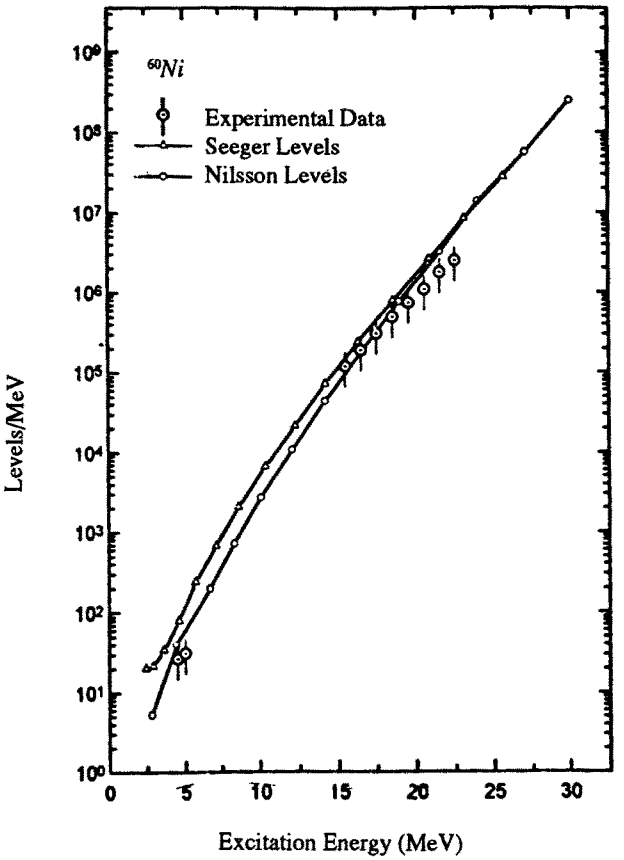

Figure 13. Same as Figure 7 for ^{60}Ni

Seeger and the Nilsson single fermion levels. The agreement for most nuclei is slightly better for the Nilsson single particle levels, whereas in a few cases the agreement is better with the Seeger single particle levels. The role of the nuclear structure effects is not directly apparent in the level density plots in Figures 7-13. For example, the contributions of the neutrons and protons to the total level density are comparable for ^{56}Fe, whereas the neutrons make a much larger contribution for ^{60}Ni. The reason for this lies in the strong participation of the highly degenerate $1g_{\frac{9}{2}}$ single particle levels in the case of ^{60}Ni.

The calculated and measured values of the spin cut-off factor σ^2 are plotted in Figure 14 for ^{56}Fe. The importance of the single particle shell structure is shown in this figure by the independent contributions of σ_n^2 and σ_p^2. It is interesting to note the proton contribution σ_p^2 dominates for Fe, whereas the situation reverses for Ni where the neutron contribution σ_n^2 dominates (Fig. 6). The result that σ_p^2 is larger than σ_n^2 for ^{56}Fe is explained by the occupational probabilities for the various single particle levels. The enhancement in σ_p^2 is mainly due to the large contribution from the $1f_{7/2}$ proton single particle levels. The addition of a few neutrons and protons in going from ^{56}Fe to ^{60}Ni completely reverses the importance of the roles of neutrons and protons. Now the $1f_{7/2}$ proton and neutron single particle levels are both nearly fully occupied and make only a minor contribution to σ^2. For ^{60}Ni, the $1g_{7/2}$ single particle levels have a sizable occupation for neutrons. Hence this level makes a major contribution to σ_n^2 resulting in a value of σ_n^2 for ^{60}Ni which is much higher than σ_p^2. The contribution of the higher angular momentum $1g_{9/2}$ single particle levels is evident also in the σ^2 values for ^{60}Ni.

In summary, by considering the effects of nuclear pairing as well as the influence of the discrete structure of single particle eigenstates on the behaviour of the nuclear state and level densities we have found that the agreement between the experimental nuclear level densities and the microscopic theory is very good, for both Seeger and Nilsson single particle fermion levels. This probability indicates that the microscopic theory provides more precise information on nuclear level density and spin cut-off factors. However, it would be worthwhile to apply the other statistical models to deduce the state and nuclear

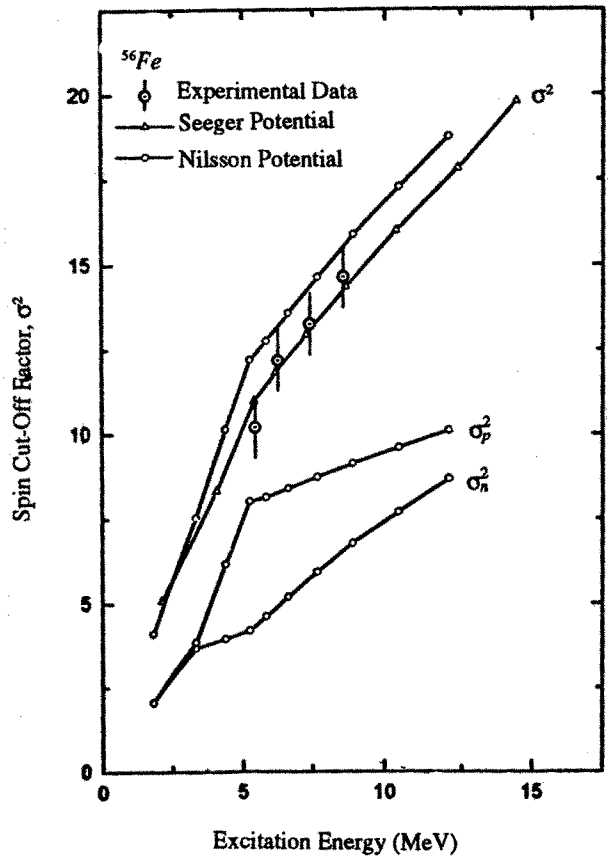

Figure 14. Comparison of the experimental spin cut-off factor for ^{56}Fe [19,20] with a microscopic theory. The calculations were performed with single particle levels of Seeger *et al.* and Nilsson *et al.* The contributions of the neutrons and protons to σ^2 for the single particle levels of Nilsson *et al.* are shown also.

level densities and compare the results with the microscopic theory. Such an investigation is, in fact, in progress.

Acknowledgements

The authors wish to thank Professor Walter Loveland for several helpful discussions. The help of the members of the Shiraz University Computer Center is also appreciated.

References

1. Weidenmuller, H.A. *Phys. Lett.*, **10**, 331, (1964).
2. Baba, H. *Nucl. Phys.*, **A159**, 162, (1970).
3. Glatz, F. *et al. Z. Phys.*, **A303**, 239, (1981).
4. Mostafa, M.G., Blann, M., Ignatuk A.V., and Grime, S.M. *Phys. Rev.*, **45**, (3), 1078, (1992).
5. Bardeen, J., Copper, L.N. and Schnieffer, J.R. *Ibid.*, **164**, 162, (1957).
6. Kargar, Z. *et al.* 9th Int. Sym. on Capture Gamma-Ray Spectroscopy. (To be published), (1996).
7. Behkami, A.N. *et al. Bull. Am. Phys. Soc.*, **41**, (5), AD13,1226, (1996).
8. Behkami, A.N. and Huizenga, J.R. *Nucl. Phys.*, **A217**, 1, (1973).
9. Behkami, A.N. and Najafi, S.I. *J. Phys. G. Nucl. Part. Phys.*, **6**, 685, (1980).
10. Behkami, A.N. and Kargar, Z. *Ibid.*, **18**, 1223, (1992).
11. Audi, G. and Wapstra, A.H. *Nucl. Phys.*, **A566**, 1, (1993).
12. Nilsson, S.G. *et al. Ibid.*, **A131**, 1, (1961).
13. Von Egidy, T., Schmidt, H.H. and Behkami, A.N. *Ibid.*, **A481**, 189, (1988).
14. Huizenga, J.R., Rossner, H.H. and Schroder, W.U. *J. Phys. Soc. JPN.*, **54**, 257, (1985).
15. Gilbert, A. *Can. J. of Phys.*, **43**, 1446, (1965).
16. Seeger, A. and Perisho, R.C. *Nucl. Phys.*, **A238**, 491, (1975).
17. Iljinov, A.S. and Mebel, M.V. *Ibid.*, **A543**, 517, (1991).
18. Beckerman, M. *Ibid.*, **A278**, 333, (1975).
19. Grimes, S.M., *et al. Phys. Rev.*, **27**, (6), 2893, (1983).
20. Fischer, R., Traxler, G., Uhi, M. and Vonach, H. *Ibid.*, **C30**, (1), 72, (1984).